Toughening Mechanisms in Commercial Thermoplastic Polyolefin Blends

J. LU,[1] G.-X. WEI,[1] H.-J. SUE,[1] J. CHU[2]

[1] Polymer Technology Center, Department of Mechanical Engineering, Texas A&M University, College Station, Texas 77843-3123

[2] Materials Engineer Department, Visteon Automotive System, Dearborn, Michigan 48121

ABSTRACT: Impact fracture mechanisms in a variety of commercially available and experimental thermoplastic polyolefin (TPO) blends were studied using the double-notch four-point-bend Charpy impact test, followed by microscopy observations. It was shown that the failure mechanisms and the sizes of the subcritically formed crack-tip damage zone before fracture were quite different among the TPO systems investigated. The room temperature Izod impact strengths of the TPOs investigated were found to correlate qualitatively well with the sizes of the damage zone. At room temperature the main fracture mechanisms observed in TPOs include matrix crazing, particle–matrix debonding, rubber particle internal cavitation, and shear banding. At low temperature (−40°C), the operative fracture mechanisms in TPOs are limited only to crazing, particle cavitation, and debonding. A strategy for improving impact strength without sacrificing scratch/mar resistance of TPOs is discussed. © 2000 John Wiley & Sons, Inc. J Appl Polym Sci 76: 311–319, 2000

Key words: thermoplastic polyolefin; toughening; fracture mechanism; impact strength; scratch/mar resistance

INTRODUCTION

Thermoplastic polyolefins (TPOs) have exhibited particularly good potential for automotive and other structural applications. They not only possess balanced physical and mechanical properties but also are inexpensive and can be recycled. However, there are still many improvements to be made to satisfy the ever-increasing demands of the automotive industry. Two properties of TPOs that need to be improved today are most low-temperature impact strength and scratch resistance.

A well-known approach to improving the impact strength of polymers is incorporating a dispersed rubbery phase.[1,2] Although there have been limited successes using rubber toughening to improve the low-temperature impact resistance of TPOs, these have been accompanied by a noticeable reduction in rigidity, which significantly lowers the scratch/mar resistance of the resulting TPO blends. This problem has hindered the growth of TPOs in the automotive industry.

The effectiveness of rubber toughening highly depends on the mechanical properties of the matrix, the modifier, the dispersion of the modifier, and the interfacial adhesion among the different phases.[1,3–8] A fundamental understanding is still lacking for TPO blends about how toughening mechanisms operate with respect to the aforementioned factors. Numerous time-consuming trial-and-error practices have been tried in the industry. A precise methodology for effective toughening of TPOs without sacrificing scratch/mar resistance is still beyond reach. In order to design TPO blends with balanced mechanical properties, it is imperative that we gain a fundamental knowledge of impact fracture behavior in

Correspondence to: H.-J. Sue.

Journal of Applied Polymer Science, Vol. 76, 311–319 (2000)

TPOs as well as in the scratch/mar damage process.

As part of a larger effort to improve both low-temperature impact strength and scratch resistance in TPOs, the focus of the present article is on studying the micromechanical deformation mechanisms in a variety of commercially available and experimental TPO blends. Since the compositions of these commercial TPOs are very complex and their exact compositions are unknown to us, it is difficult to determine precisely the cause or causes for the occurrence of a specific toughening mechanism. Nevertheless, it is possible to identify the dominant toughening mechanisms, the critical conditions for these mechanisms to operate, and the factors that affect the toughening process. The purpose of studying these commercial and semicommercial TPOs is to gain valuable insight into the toughening mechanisms in these relatively successful commercial TPOs and to use that insight as a reference for future fundamental investigations on model TPO blends. In this study, the DN-4PB-CI method[9] was employed and followed by various microscopy observations.

EXPERIMENTAL

Materials

Two commercially available TPOs and one experimental TPO were chosen for the present study. The commercially available TPOs are TSOP-5 from Toyota (designated as T-TPO) and XFBR712 from Montell (designated as M-TPO). The experimental TPO is an elastomeric polyethylene-toughened PP (designated as D-TPO), which was provided by Dow Chemical Company. These three TPOs have tensile moduli of about 1.8 GPa. Since these TPOs are either commercially available or to be used as a commercial product, their compositions are not revealed by the suppliers.

The Double-Notch Four-Point Bend Charpy Impact Test

Injection-molded specimens with dimensions of 12.7 cm × 1.27 cm × 0.375 cm (5″ × 0.5″ × 0.125″), received from the commercial sources, were notched using a notching cutter with a 250-μm tip radius to cut a notch with a depth of 0.375 cm (0.125″) for the blunt crack DN-4PB-CI experiment. The distance between the two notches on the DN-4PB-CI bar was set at 1.12 cm (0.44″) to ensure that the two cracks propagated independently from each other (Fig. 1). In the case of the sharp crack DN-4PB-CI experiment, sharp cracks were generated via a liquid nitrogen–chilled razor blade tapped at the notch tips. The ratio between the final crack length and the specimen width was held in a range between 0.3 and 0.6. The DN-4PB-CI test was performed on a pendulum impact tester (Model TMI-43-02) with a modified double-head striker (Fig. 1). In the case of the low-temperature DN-4PB-CI tests, the specimens and the support were conditioned in an environmental chamber with a temperature setting of −40°C for at least 20 min. Subsequently the chamber cover was opened, and the impact test was conducted immediately.

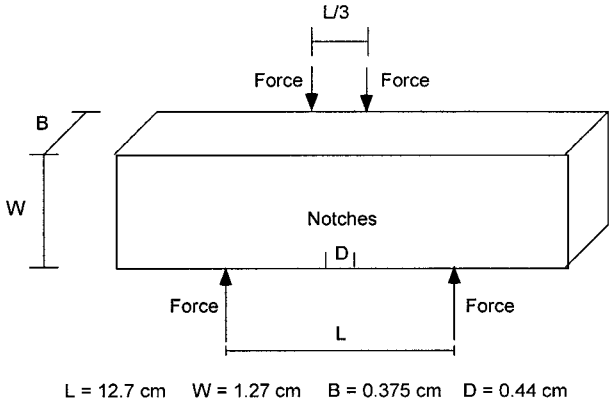

Figure 1 Schematic of the DN-4PB geometry.

Microscopy Investigations

Using a diamond saw, the damage zone around the subcritically propagated DN-4PB-CI crack was cut into two halves along the crack propagation direction, but perpendicular to the fracture surface (Fig. 2). The plane strain core sides of the surface were prepared for optical microscopy (OM) and transmission electron microscopy (TEM) investigations. In the OM investigation, thin sections, ranging from 40 to 100 μm, of the tested DN-4PB-CI specimens were obtained by polishing, following the procedure described by Holik et al.[10] The thin sections were then examined using an Olympus BX60 optical microscope and a Nikon SMZ-10 stereo microscope.

In the TEM experiment the core region of the damage zone was carefully trimmed to an area of about 5 mm × 5 mm and embedded in DER 331 epoxy–diethylenetriamine (12:1 ratio by weight).

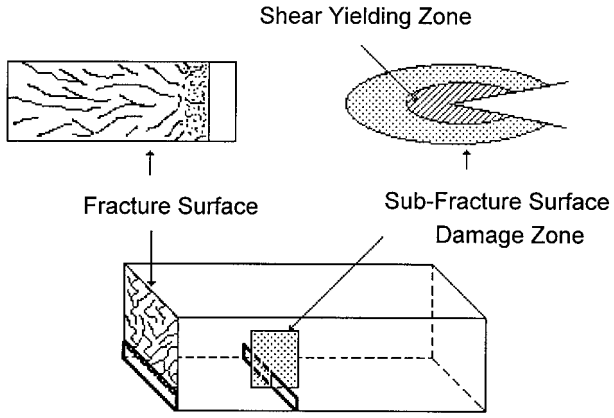

Figure 2 Schematic of the DN-4PB damage zones used for TOM and TEM investigations.

The epoxy was cured at room temperature for 16 h. The cured block was further trimmed to a size of about 0.3 mm × 0.3 mm, with the desired damage region roughly at the center of the trimmed surface. A glass knife was used to face off the trimmed block cryogenically prior to RuO_4 staining. The faced-off block was exposed overnight to the vapor of a solution containing 0.2 g of $RuCl_3$ and 10 mL of 5.25% aqueous sodium hypochlorite. Ultrathin sections, ranging from 60 to 80 nm, were obtained using a Reichert-Jung Ultracut E microtome with a diamond knife. The thin sections were placed on 100-mesh Formvar-coated copper grids and examined using a Zeiss-10C TEM operated at an accelerating voltage of 100 kV.

RESULTS

Room Temperature Impact Tests

For all three samples investigated, stress-whitened zones were found around the DN-4PB-CI arrested subcritically propagated crack at room temperature. Optical stereomicroscopy gives an overview of the damaged areas (Figs. 3 and 4). Under transmitted light, the damage zone is shown to be much darker than the undamaged area. This indicates that widespread cavitation, which scatters light effectively, has taken place in the damage zone. The room temperature Izod impact strengths of M-TPO, T-TPO and D-TPO were found to be 42.6 kJ/m^2, 29.5 kJ/m^2, and 36.8 kJ/m^2, respectively.[11] It appears that, at least qualitatively, the room temperature Izod impact strength of these TPOs is related to the size of the damage zone observed.

TOM further revealed the fracture mechanisms in the TPO systems. The bright field micrographs of the three samples are shown in Figure

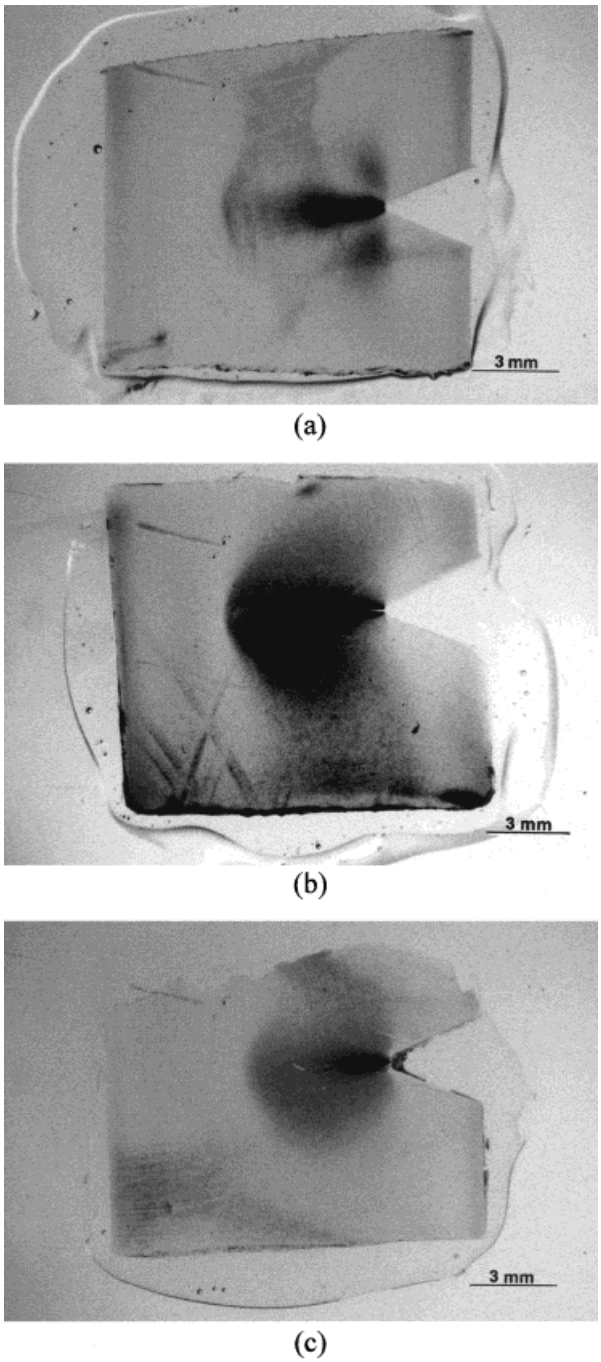

Figure 3 Transmitted optical stereomicrographs of room temperature blunt crack DN-4PB-CI damage zones: (a) D-TPO, (b) M-TPO, and (c) T-TPO. The crack propagates from right to left.

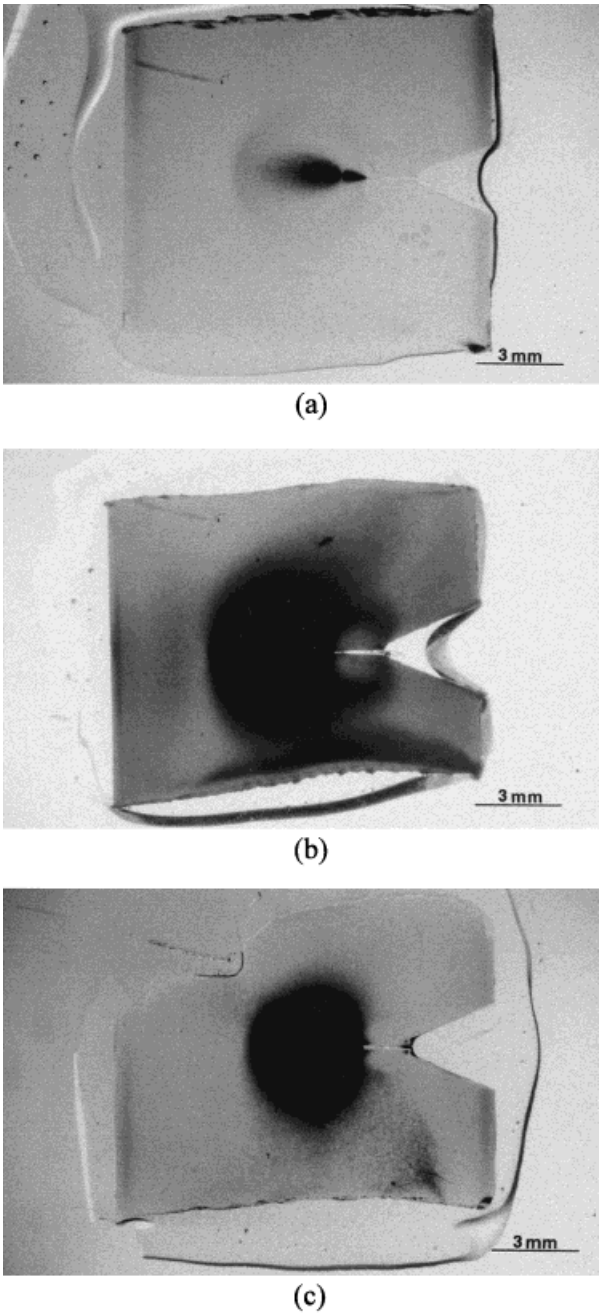

Figure 4 Transmitted optical stereomicrographs of room temperature sharp crack DN-4PB-CI damage zones: (a) D-TPO, (b) M-TPO, and (c) T-TPO. The crack propagates from right to left.

5. The cavitation phenomenon is clearly seen. The D-TPO system shows a typical crazing pattern. When the damage zones are viewed under crossed polars, significant birefringence is found for all three TPOs (Fig. 6). This suggests that shear banding must have occurred inside the damage zones of these TPOs.

TEM was utilized to probe the detailed toughening mechanisms and morphological features in the TPOs. TEM micrographs of the three TPOs

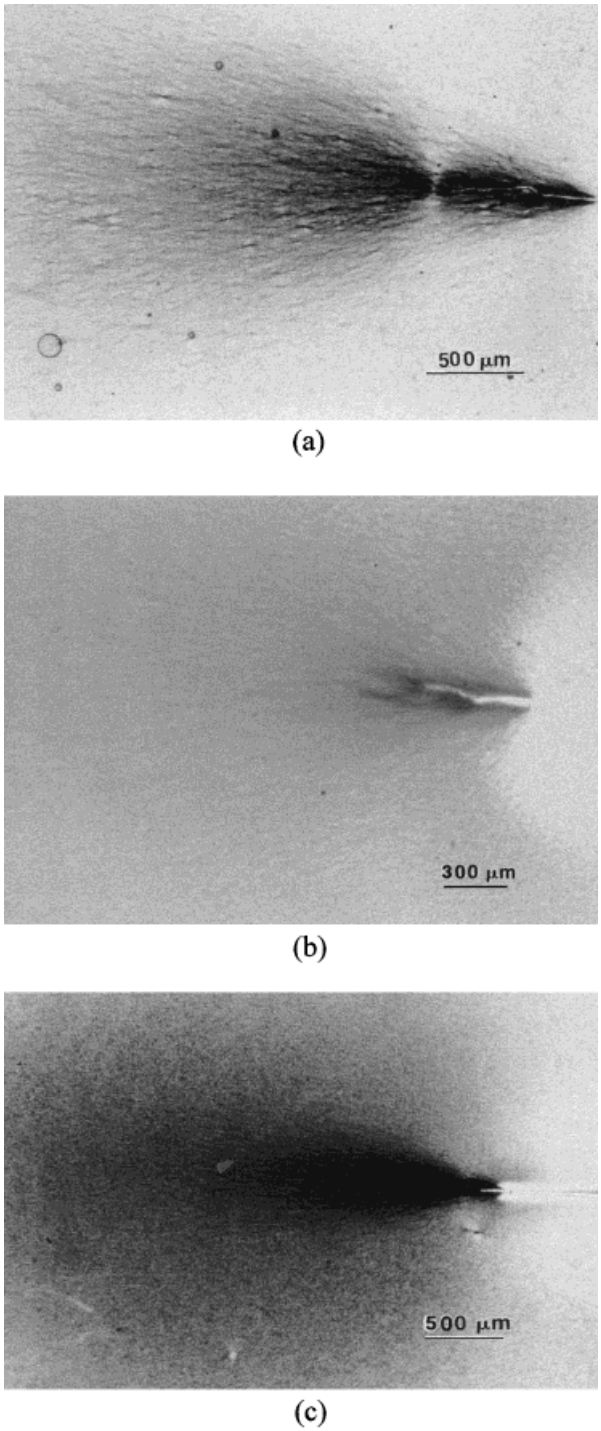

Figure 5 Bright field TOM micrographs of room temperature sharp crack DN-4PB-CI damage zones: (a) D-TPO, (b) M-TPO, and (c) T-TPO. The crack propagates from right to left.

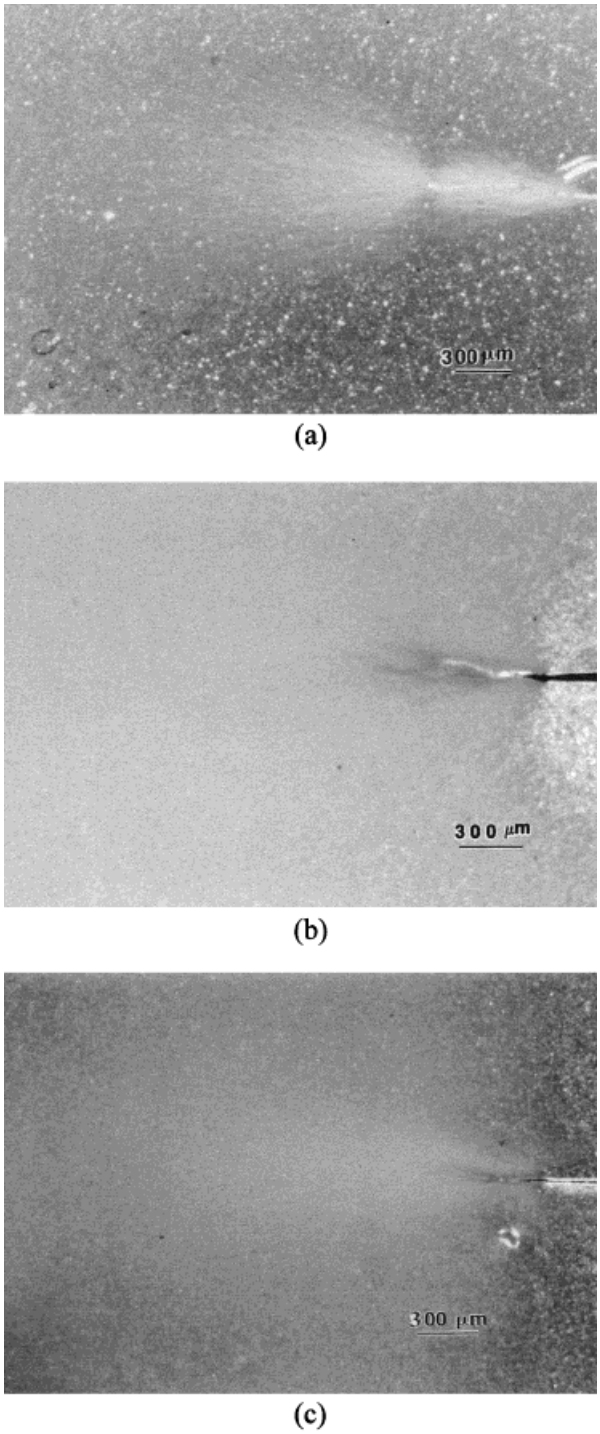

Figure 6 Cross polarization TOM micrographs of room temperature sharp crack DN-4PB-CI damage zones: (a) D-TPO, (b) M-TPO, and (c) T-TPO. The crack propagates from right to left.

taken inside the DN-4PB damage zone are shown in Figures 7–9. The TEM micrographs indicate that crazes are formed in all three TPOs but at

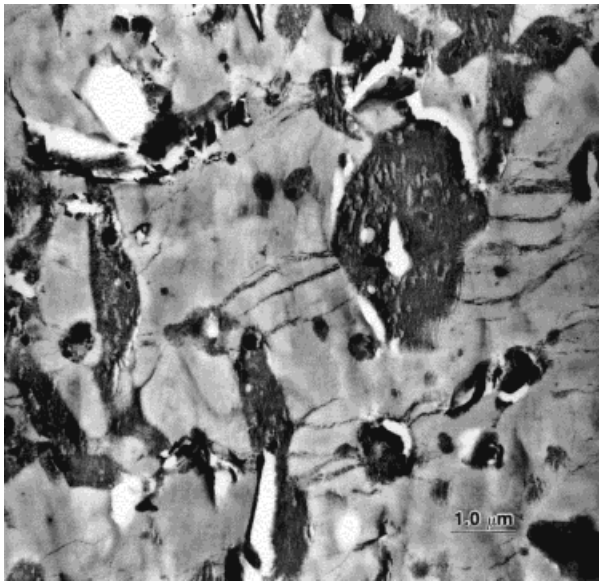

Figure 7 TEM micrograph of the room temperature sharp crack DN-4PB-CI damage zone of D-TPO. The crack propagates from right to left.

different levels. M-TPO and D-TPO exhibit a high intensity of crazing, while T-TPO only has a little sign of crazing, if any. Some amount of rubber-particle cavitation and filler particle–matrix debonding are also observed in these samples. However, because of the presence of complex morphology in these TPOs, it is not entirely clear

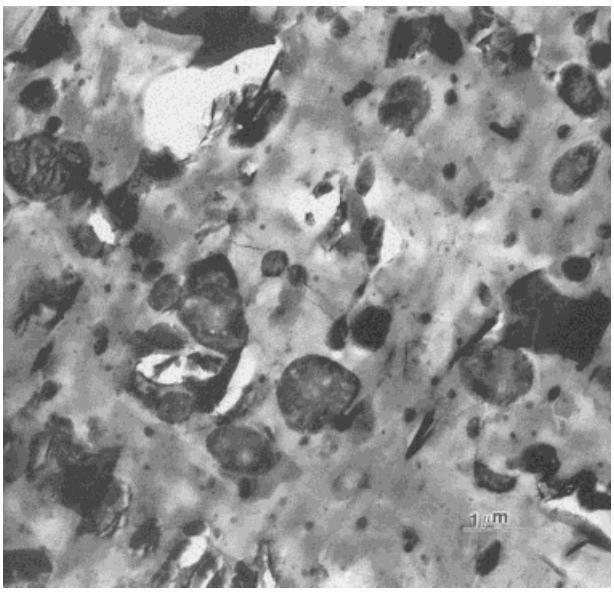

Figure 8 TEM micrograph of the room temperature sharp crack DN-4PB-CI damage zone of T-TPO. The crack propagates from right to left.

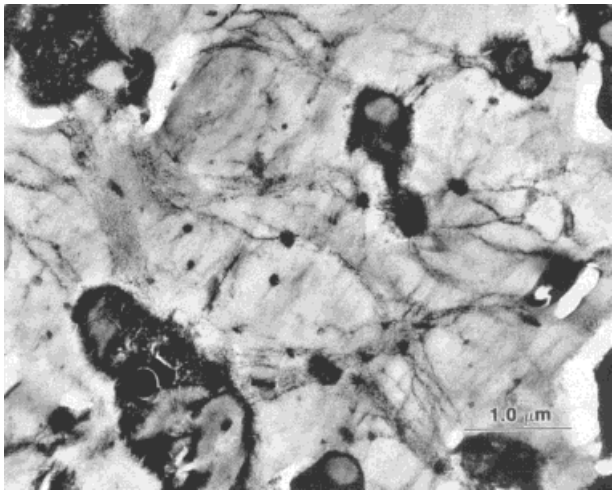

Figure 9 TEM micrograph of the room temperature sharp crack DN-4PB-CI damage zone of M-TPO. The crack propagates from right to left.

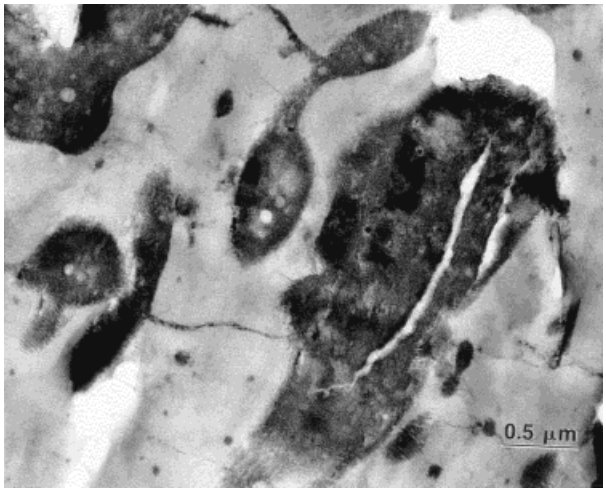

Figure 10 TEM micrograph, taken at a higher magnification than Figure 7, of the room temperature sharp crack DN-4PB-CI damage zone of D-TPO. It is evident that the rubber-particle phase in D-TPO and T-TPO cocrystallizes well with the PP matrix.

whether these rubber-particle cavitation and filler particle–matrix debonding phenomena are partially due to microtoming.

From TEM it is evident that all three TPO systems contain rubber particles and inorganic fillers. The dispersion of the rubber particles is rather good in all three TPOs. The rubber-particle morphology in M-TPO is quite different from that in D-TPO and T-TPO. In M-TPO, each of the rubber particles in M-TPO contains one or several semicrystalline inclusions surrounded by an amorphous rubbery phase (Fig. 9). This surrounding amorphous phase, which is speculated to be ethylene-propylene-block copolymer, provides a good interfacial adhesion between the semicrystalline inclusions and the TPO matrix. Compared with M-TPO, D-TPO and T-TPO have a quite uniform rubber-particle morphology. It is interesting to note that the rubber-particle phase in D-TPO and T-TPO cocrystallizes well with the PP matrix (Figs. 10–11), which may also result in a rather strong interfacial bonding between the rubber and the matrix.

Low-Temperature Impact Tests

Under low-temperature impact (−40°C), the sharp crack DN-4PB-CI tests give no significant damage zone around the subcritically propagated crack for all three TPOs. For the blunt crack impact fracture tests at −40°C, the three TPO samples behave differently. D-TPO appears to undergo crazing [Fig. 12(a)]. M-TPO appears to undergo a cavitation or a debonding type of damage [Fig. 12(b)]. No significant damage zone was found around the arrested crack of T-TPO [Fig. 12(c)]. For all three samples, no sign of birefrin-

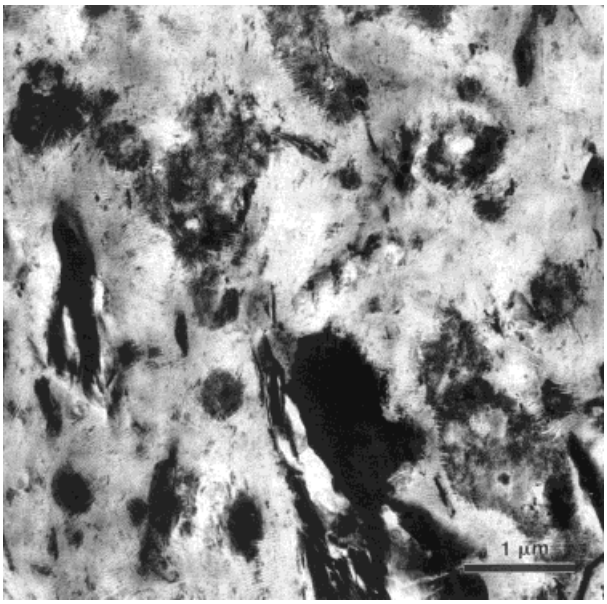

Figure 11 TEM micrograph, taken at a higher magnification than Figure 8, of the room temperature sharp crack DN-4PB-CI damage zone of T-TPO. It is evident that the rubber-particle phase in D-TPO and T-TPO cocrystallizes well with the PP matrix.

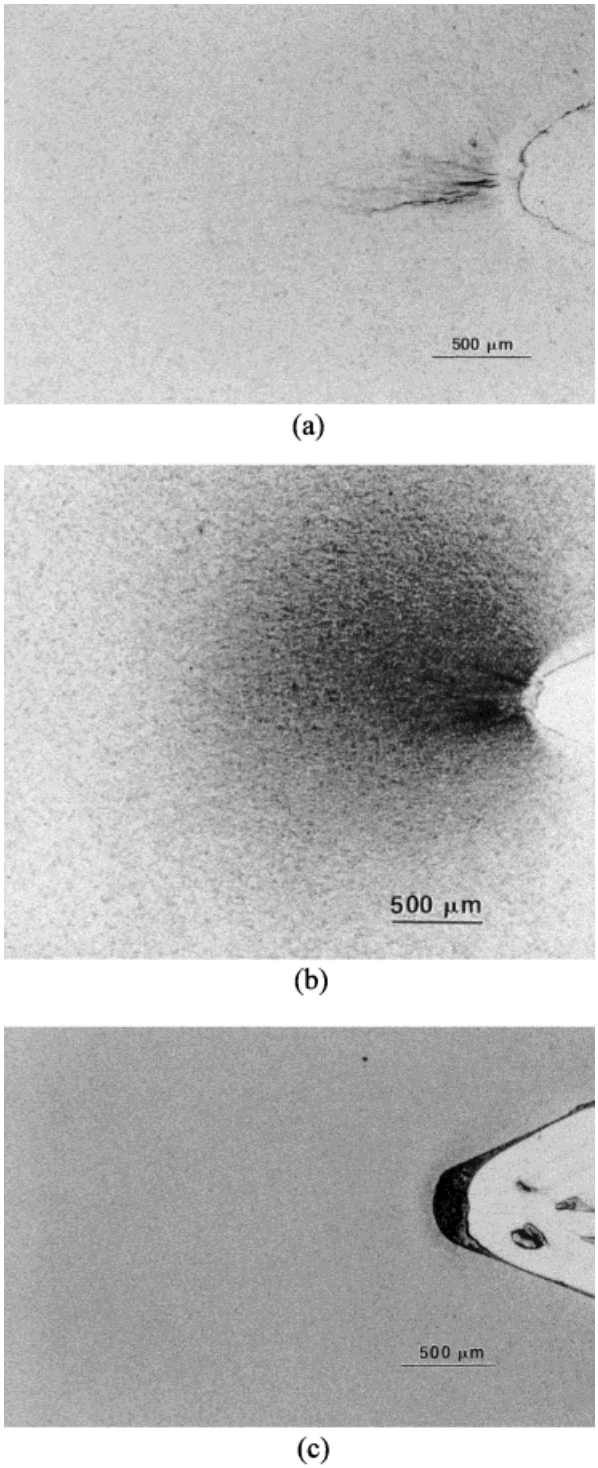

Figure 12 Cross polarization TOM micrographs of the low-temperature blunt crack DN-4PB-CI damage zones: (a) D-TPO, (b) M-TPO, and (c) T-TPO. The crack propagates from right to left.

gence was observed around the arrested cracks. The shear banding mechanism is suppressed at −40°C.

DISCUSSION

To toughen a given polymer, the promotion of effective energy-dissipating fracture mechanisms is required. There are many types of possible toughening mechanisms for polymers. Each type of toughening mechanism has its critical condition or conditions for operation. The role of tougheners is to induce extensive micromechanical toughening mechanisms.

Optical microscopy shows that widespread cavitational mechanisms take place in the DN-4PB damage zones at room temperature. Possible cavitation mechanisms include matrix crazing, rubber-phase cavitation, and/or filler particle–matrix debonding. TEM observations indicate that different TPO systems exhibit distinctly different cavitational processes. M-TPO and D-TPO undergo extensive matrix crazing upon impact damage, while T-TPO shows little sign of crazing, if any. The cavitational mechanisms that occurred in T-TPO appear to be mainly rubber-phase cavitation and/or filler particle–matrix debonding.

For crazing to occur, a high level of hydrostatic tension needs to exist ahead of the crack tip. The TEM micrographs suggest that a good interfacial adhesion exists between the toughener particles and the matrix in all the TPO systems studied. Good interfacial adhesion can help promote a high magnitude of hydrostatic tension around the crack tip.[12] This is favorable for the formation of crazing. However, whether crazing occurs also depends on the nature of the toughener phase and the matrix, as well as on the dispersion of the toughener. In this study different intensities of crazing have been observed in the three TPOs. Speculation is that the difference in the TPO matrix composition could be a reason for the different crazing intensities.

From TEM micrographs taken in the damage zones of M-TPO and D-TPO (Figs. 7 and 9), we can see that crazes start at the rubber–matrix interface, propagate through the matrix, and terminate at the surrounding rubber particles. This indicates that the rubber phase acts not only as a stress concentrator but also as a craze stabilizer to help prevent crazes from transforming into premature cracks that could lead to catastrophic failure.

For all TPO samples tested at room temperature, TOM shows that inside a larger diffusive damage zone there is an intensive deformation zone around the arrested crack tip (Fig. 6). Under crossed polars, the intensive deformation zone is

birefringent, indicating the presence of shear banding mechanism. When a specimen with a crack is subjected to a far field tensile stress perpendicular to the crack, there will exist a state of triaxial tension ahead of the crack tip. It has been suggested that the triaxial tension at the crack tip has to be relieved in order for the remaining deviatoric stress to reach a critical value for shear yielding.[13,14] Crazing, debonding, and internal cavitation of toughener phase are dilatational types of damage mechanisms. Once these dilatational mechanisms become operative, the stress state in the matrix can be converted from triaxial to a more biaxial or uniaxial stress state. The relief of triaxial tension will facilitate shear yielding because the deviatoric stress remains high.[13,14] For this reason, the TPO samples in this study undergo massive matrix shear yielding after the cavitational processes. In this regard, others have already observed the phenomenon of the transformation of a crazed zone into a shear-yielded zone in thermoplastic polymer blends.[15,16]

For thermoplastics, crazing and shear yielding are the most frequently encountered energy dissipation mechanisms.[15] They are also the two most effective energy dissipation mechanisms. In M-TPO and D-TPO, both massive crazing and massive shear yielding took place during room temperature impact damage. In T-TPO massive crazing did not occur, but massive shear yielding was still triggered by other cavitational mechanisms. However, an impact strength that was relatively lower was obtained for T-TPO, unlike for M-TPO and D-TPO, possibly due to the lack of massive matrix crazing. The impact fracture toughness is determined by many factors, including the nature of the matrix, the type of modifier, the size and phase morphology of modifier particles, interparticle distance, and the interfacial adhesion between the modifier particles and the matrix, etc. These factors may interact with one another. A synergism among them may be present. Therefore, it will be hard to isolate the influence of each individual factor on the fracture behavior in the above commercial and semicommercial TPO systems.

At −40°C, most toughening mechanisms, especially the shear yielding mechanism, are suppressed. As a result, the fracture toughness decreases significantly. Nevertheless, it should be noted that the properties of the matrix and the modifier as well as the interfacial adhesion between the two phases may all change as the temperature decreases. Hence, it is imperative to discover an approach that promotes effective toughening mechanisms at low temperatures.

A common problem accompanying rubber toughening is the reduction in modulus, which significantly lowers the scratch resistance of the toughened systems. In commercial TPO blends, rigid inorganic fillers, such as talc, are usually added to improve rigidity in hopes of increasing scratch resistance. However, the interfacial adhesion is usually poor between talc and TPO. On scratching the TPO surface, debonding will take place across the TPO surface and cause visible scratches and mars to appear. Furthermore, inorganic fillers are usually used at low levels in order to retain high toughness of TPOs. As a result, using inorganic fillers to improve scratch resistance is not an effective approach.

The recent introduction of the rigid–rigid polymer-toughening concept[15–18] has provided a new route for developing TPO blends with both high impact fracture toughness and good scratch resistance. This concept suggests that as long as the rigid toughener phase can (1) generate numerous stress concentration sites around the crack tip and (2) relieve the triaxial tension in front of the crack tip, the matrix can be toughened by the dispersion of the second-phase rigid polymer. This makes it possible to improve both the toughness and modulus of TPOs by incorporating rigid engineering thermoplastic polymers such as polycarbonate, polyethylene terephthalate, and polyphenylene oxide. Investigation of the rigid–rigid polymer toughening of TPOs is underway and will be published shortly.

CONCLUSIONS

Room-temperature and low-temperature (−40°C) impact fracture mechanisms in a variety of commercial and semicommercial TPO blends were investigated. The size of the damage zone observed using the DN-4PB-CI tests was found to be qualitatively proportional to the Izod impact strength of the TPOs. The room temperature toughening mechanisms among these TPO systems were found to be similar. The main toughening mechanism is the widespread cavitational process or processes, followed by shear banding. Massive matrix crazing is the dominant cavitational deformation mechanism in M-TPO and D-TPO, while rubber-phase cavitation and filler particle–matrix debonding are the main cavitation mechanisms in T-TPO. The massive matrix

crazing appears to make a large contribution to the toughening. The low-temperature fracture behaviors of these TPO systems, however, differ significantly from one another and from those observed at room temperature. At −40°C, the operative fracture mechanisms are limited to crazing, particle cavitation, and/or particle debonding. The rigid–rigid polymer toughening of TPOs is currently being explored for improving both impact strength and scratch/mar resistance.

The authors would like to thank E. I. Garcia-Meitin and H. Sittertz-Bhatkar for their assistance with the TEM work.

REFERENCES

1. Bucknall, C. B. Toughened Plastics; Applied Science: London, 1977.
2. Kinloch, A. J.; Young, R. J. Fracture Behavior of Polymers; Elsevier Applied Science Publisher: London, New York, 1983.
3. Newman, S. Rubber Modification of Plastics in Polymer Blends; D. R. Paul, Ed.; Academic Press: New York, 1980; Chapter 13, Vol. 2.
4. Wu, S. Polymer 1985, 26, 1855.
5. Evans, A. G.; Ahmad, Z. B.; Gilbert, D. G.; Beaumont, P. W. R. acta metall 1986, 34, 79.
6. Kinloch, A. J.; Shaw, S. J.; Tod, D. A.; Hunston, D. L. Polymer 1983, 24, 1341.
7. Borggreve, R. J. M.; Gaymans, R. J.; Schuijer, J.; Ingen Housz, J. F. Polymer 1987, 28, 1489.
8. Breuer, H.; Haaf, F.; Stabenow, J. J Macromol Sci-Phys 1977, B14(3), 387.
9. Sue, H.-J.; Pearson, R. A.; Parker, D. S.; Huang, J.; Yee, A. F. Polym Prepr 1988, 29, 147.
10. Holik, A. S.; Kambour, R. P.; Hobbs, S. Y.; Fink, D. G. Microstruct Sci 1979, 7, 357.
11. Provided by manufacturers.
12. Durst, R. R.; Griffith, R. M.; Urbanic, A. J.; Van Essen, W. J. ACS Div Org Coat Plast Prepr 1974, 34, 320.
13. Yee, A. F.; Pearson, R. A. J Mater Sci 1986, 21, 2462.
14. Pearson, R. A.; Yee, A. F. J Mater Sci 1986, 21, 2475.
15. Sue, H.-J.; Yee, A. F. J Mater Sci 1989, 24, 1447.
16. Sue, H.-J.; Yee, A. F. J Mater Sci 1991, 26, 3449.
17. Yee, A. F.; Parker, D. S.; Sue, H.-J.; Huang, I.-C. Polym Prepr 1987, 57, 417.
18. Sue, H.-J.; Yee, A. F. SPE-RETEC (Chicago), 1987.